Proceedings of the 21st ICSMGE, Vienna, Austria, 14 – 19 June 2026. Pistrol, Adam & Schweiger (eds.)
Published by: ÖGG, Austrian Society for Geomechanics, Salzburg, Austria, ISBN 978-3-9503898-4-5
https://doi.org/10.53243/ICSMGE2026-304

Advanced Soil Constitutive Models for Predicting Seismic Responses in Soil-Pile-Superstructure Interaction

Mehdi Joneidi, Gertraud Medicus *Institute of Infrastructure, Numerical and Experimental Soil Mechanics, Universität Innsbruck, Austria, mehdi.joneidi@uibk.ac.at*

Roshanak Shafieiganjeh
ILF Consulting Engineers Austria GmbH, Department for Geotechnical Engineering, Vienna, Austria

Iman Bathaeian
Austria KELAG-Kärntner Elektrizitäts-Aktiengesellschaft, Klagenfurt am Wörthersee, Austria

Barbara Schneider-Muntau
Institute of Infrastructure, Numerical and Experimental Soil Mechanics, Universität Innsbruck, Austria

ABSTRACT: Advanced constitutive models are necessary for effective simulation and validation with laboratory and field observation to capture the realistic response of granular soils. In recent decades, considerable efforts have been made to improve soil constitutive models using various concepts. Two different frameworks which are in increasing demand in development and application are SANISAND and hypoplasticity. This study highlights the capabilities of three advanced soil constitutive models–SANISAND and two versions of hypoplasticity–in predicting the seismic responses of soil-pile-superstructure interactions under scaled input ground motions. A new version of the hypoplastic model, with three modifications proposed by Liao et al. (2024) for undrained monotonic loading, is combined with the intergranular strain concept to enhance its predictive efficacy for cyclic and seismic loading. By controlling the nonlinear term of the hypoplastic model during undrained loading, the model can mitigate the sharp increase in pore water pressure in the first cycle during the seismic loading. Further, a 3D finite element model consisting of a soil-pile superstructure is developed using ABAQUS finite element code as a boundary value problem. The soil-pile superstructure is simulated as a case study to validate the advanced models against centrifuge test data according to Wilson (1998), capturing the dynamic response of the soil and the structure. The results clearly illustrate that the extended hypoplastic model better estimates the excess pore water pressure during seismic loading and improves its ability to capture the superstructure responses, including peak values and variation trends. Additionally, the extended model addresses the shortcoming of the hypoplastic model, which often overestimates shear strain in cyclic loadings.

KEYWORDS: Hypoplasticity, SANISAND, seismic loading, pore pressure, bending moment.

1 INTRODUCTION

Predicting the dynamic behavior of soil–structure interaction remains a challenging task in earthquake geotechnical engineering. The complexity arises from the highly nonlinear and stress-dependent characteristics of both soil and structural systems during seismic loading. Traditional soil models–such as linear, equivalent linear, and fundamental elastoplastic models like the Mohr–Coulomb model–frequently inadequately predict essential characteristics including stiffness degradation, strain-rate dependence, hardening, and liquefaction phenomena. To overcome these limitations associated with granular soils, various advanced soil constitutive models have been introduced and refined to enhance the predictive accuracy of simpler models under cyclic loading conditions (Niemunis & Herle, 1997; Fuentes & Triantafyllidis, 2015; Liao et al., 2024; Tafili et al., 2024; Dafalias & Manzari, 2004; Petalas et al., 2020; Yang et al., 2022; Reyes et al., 2025). The SANISAND model (Dafalias & Manzari, 2004) and the hypoplastic model (Wolffersdorff, 1996) are frequently employed among advanced soil models due to their precise predictions of the behavior of granular soils under diverse loading conditions. Nonetheless, the hypoplastic model exhibits constraints under undrained loading conditions. It particularly overestimates pore water pressure in the initial loading phase and underestimates hardening rates during shearing. Liao et al. (2024) proposed an augmented version of the hypoplastic model to improve its efficacy under undrained monotonic loading. The validation and extension of advanced soil models have often been limited to single-element tests. In recent years, many studies have focused on validating the practical application of advanced soil models. However, further research is still required to evaluate their performance in boundary value problems and to demonstrate their reliability and applicability in real-world engineering practice. Machaček et al. (2021) and Lascarro et al. (2024) recently conducted studies in which they assessed advanced constitutive soil models through laboratory tests and simulations. Both works highlight that intergranular strain-based hypoplastic models, especially those incorporating anisotropy (HP+ISA), provide improved predictions of soil behavior under cyclic and seismic loading conditions. Additionally, the results of the soil-pile interaction analysis showed that the hypoplastic model and SANISAND adequately captured the pore water pressure buildup during vibratory pile driving. However, these models had difficulty accurately predicting the amplitude of this pressure (Machaček et al., 2021). This paper examines the predictive capabilities of three advanced constitutive models based on two key theoretical frameworks: hypoplasticity and the bounding surface model. Two hypoplastic models (Wolffersdorff, 1996; Liao et al., 2024) that incorporate the intergranular strain concept (Niemunis & Herle, 1997) and the SANISAND model (Dafalias & Manzari, 2004) are employed to simulate soil-pile-superstructure interaction (SPSI) under two scaled ground motions from the Kobe earthquake and investigate the seismic performance of these models. In this paper, a 3D numerical analysis is performed using ABAQUS/Standard software to compare the simulation results with those from a physical model test conducted by Wilson in 1998.

2 EXPERIMENTAL TEST

This paper evaluates the effectiveness of three advanced constitutive soil models for predicting the seismic response of soil-pile interactions based on centrifuge tests conducted by Wilson (1998). The experiments investigated the dynamic behavior of soil–pile–superstructure systems in a bilayer liquefiable soil profile. Earthquake loading was applied via servo-hydraulic actuators, starting with low-level motions to observe small-strain responses, using recorded Kobe earthquake data at a centrifuge acceleration of 30 g, representing a scale factor of 30 (Wilson, 1998). Figure 1 demonstrates the spectral response of input ground motions from the Kobe earthquake for two scaled PGA levels. The physical model consisted of saturated Nevada sand layers: a 9.3 m - thick medium-dense upper layer (relative Density, D_{r0}, of 55%) and an 11.4 m - thick dense lower layer (relative Density, D_{r0}, of 80%). The centrifuge test instrumentation in this study included strain gauge and pore pressure sensors. A single aluminum pile (Diameter, D = 0.67 m, wall thickness = 72 mm) extended 20.6 m in total - with 3.8 m above ground - and was topped with a 49.1 t superstructure to replicate structural loading.

3 SOIL CONSTITUTIVE MODELS

3.1 *Hypoplastic models*

The hypoplastic model, originally proposed by Kolymbas (1977), is a type of nonlinear soil model. Unlike traditional models, the hypoplastic model does not depend on ideas from elastoplastic theory, such as yield surfaces, hardening laws, flow rules, and the division of strain into elastic and plastic parts. A notable hypoplastic (HP) model frequently utilized by numerous researchers is the one proposed by Wolffersdorff (1996), which is regarded as a fundamental hypoplastic model for its subsequent extensions. The model was initially developed for monotonic loading conditions. Subsequently, it was extended by Niemunis & Herle (1997) and enhanced by the intergranular strain (IGS) concept, which was applied to both loading and unloading conditions. In the present study, the aforementioned model is referred to as HP+IGS in the context of numerical results description. The hypoplastic model that includes intergranular strain effects (HP+IGS) comprises thirteen material parameters–eight pertaining to the HP model and five related to the intergranular strain concept. The HP (Wolffersdorff, 1996) model, despite its ability to accurately reproduce soil behaviour under drained conditions, frequently exhibits deficiencies in undrained monotonic loading conditions. Liao et al. (2024) initially proposed a modified hypoplastic model (MHP). To enhance the model's capacity to accurately capture limited flow behavior and prevent overestimation of mean effective stress degradation and strain accumulation during cyclic loading, three key modifications were implemented by Liao et al. (2024). In this modification, the nonlinear part of the hypoplastic model is turned off at first, leading to a completely elastic response at the beginning of undrained shearing. In contrast to the behavior observed in drained conditions, undrained loading tests are assumed to show a predominance of elastic strains, resulting in a fully elastic response during the initial loading stage (Liao et al. 2024). In this paper, a new combination of a MHP (Lia et al. 2024) with the IGS concept (MHP+IGS) is used as the second constitutive model in finite element analysis. The MHP+IGS model incorporates an additional five input parameters into the hypoplastic framework. Table 1 presents the parameters used for numerical simulations with the HP+IGS and MHP+IGS models.

Table 1. Parameters used in the HP+IGS and MHP+IGS models for Nevada Sand, (adapted from Liao et al., 2024; Joneidi et al., 2025).

Soil model	Index	HP+IGS	MHP+IGS
Wolffersdorff (1997) HP model	φ_c (°)	31°	31°
	h_s (MPa)	4000	4000
	n	0.30	0.30
	e_{c0}	0.887	0.887
	e_{d0}	0.511	0.511
	e_{i0}	$1.15e_{c0}$	$1.15e_{c0}$
	α	0.40	0.40
	β	1	1
IGS parameters	R	0.0001	0.0001
	m_R	5	5
	m_T	2	2
	β_r	0.20	0.20
	χ	3	3
MHP model	λ_1, λ_2	-	0.40, 2.5
	e_{l0}	-	0.10
	k_l	-	12
	μ_0	-	1.30

3.2 *SANISAND model*

The SANISAND model, developed by Dafalias and Manzari (2004), considers fabric changes during the dilative phase of deformation. These changes influence the subsequent contractive response of the soil during unloading. As a bounding surface plasticity model, SANISAND uses four conical surfaces in deviatoric stress space: a yield surface (centered on the back-stress ratio α) which is governed by kinematic hardening, a bounding surface, a dilatancy surface, and a critical state surface. A mapping rule regulates loading and unloading behavior by relating the current back-stress ratio to its corresponding points on the bounding and dilatancy surfaces. SANISAND builds on an earlier two-surface plasticity framework by incorporating the evolution of the fabric-dilatancy tensor during dilation, which enables more accurate simulation of soil behavior under cyclic loading. In this study, the SANISAND model was also used to simulate the behavior of liquefiable Nevada sand under seismic loading, and its predictive performance was compared with the two versions of the hypoplasticity model. The SANISAND model is characterized by fourteen independent parameters that control its elastic response, critical state behavior, yield surface, plastic modulus, dilatancy, and the fabric–dilatancy relationship (see Table 2). The input parameters for the three mentioned soil models were calibrated using undrained triaxial monotonic and cyclic compression tests, which were conducted under varying initial confining pressures. Detailed descriptions of the calibration process and the formulation of the three applied soil models can be found in Joneidi et al. (2025).

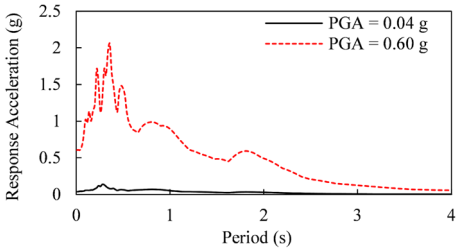

Figure 1. Spectral response of the Kobe earthquake for PGA = 0.04 g and 0.6 g, data from Wilson (1998).

Table 2. SANISAND parameters for Nevada Sand (adapted from Taiebat et al., 2010; Joneidi et al., 2025).

	Index	Value [unit]
Elasticity	G_0	200 [-]
	ν	0.05 [-]
Critical state	M_c	1.24 [-]
	M_e	0.88 [-]
	λ_c	0.027 [-]
	e_0	0.83 [-]
	ξ	0.45 [-]
Yield surface	m	0.02 [-]
Plastic modulus	h_0	9.70 [-]
	c_h	1.02 [-]
	n_b	2.56 [-]
Dilatancy	A_0	0.81 [-]
	n_d	1.05 [-]
Fabric-Dilatancy-tensor	z_{max}	5.00 [-]
	c_Z	800 [-]

4 NUMERICAL SIMULATION

Three-dimensional numerical simulations were conducted using the finite element software ABAQUS [1]. Given that seismic loading was applied uniaxially and the out-of-plane response was minimal, only half of the model geometry is simulated to reduce computational time (Figure 3). Based on the centrifuge test report, the saturation densities ρ for the medium-dense and dense sand layers were 1.95 and 1.99 kg/cm³, respectively, with corresponding initial void ratios e_0 of 0.686 and 0.592. The single pile was modeled as a hollow aluminum alloy tube (6061-T6), with a unit weight of 2.7 t/m³, a Poisson's ratio of 0.33, and a bending stiffness of 427 MN·m². The pile behavior was defined using an elastic–perfectly plastic model governed by the von Mises yield criterion, assuming a yield strength of 290 MPa. To reduce boundary effects, the lateral model boundaries were extended approximately 36 times the pile diameter (36D) in both x and y directions, significantly exceeding the 12D spacing recommended in (Kotronis & Escoffier 2014). The soil and pile were discretized using eight-node, fully integrated, linear brick C3D8 elements. The numerical model used a maximum soil element size of 1 m at depth and finer mesh elements of 25 cm in the vicinity of the pile to capture local stress variations more accurately. The single pile was discretized into 336 elements with a minimum size of 0.4 m distributed along its entire length. The superstructure was simplified as a lumped mass located at the pile head. The simulation proceeded in three sequential stages: geostatic, static general, and implicit dynamic analysis. The geostatic step defined the initial stress field, and the static general step activated the pile. During the geostatic stage, the bottom boundary was fixed to replicate the presence of bedrock, and the external soil surfaces were constrained vertically along the x and y axes. At the onset of the dynamic phase, the x-direction restraint at the base was removed, and the input seismic acceleration time history was applied. To mitigate wave reflection from the model boundaries, the vertical surfaces perpendicular to the shaking direction were constrained using a Multiple Point Constraint (MPC) scheme. This approach ties corresponding nodes on opposing vertical boundaries at the same depth, effectively simulating laminar boundary conditions. A free-drainage condition was applied at the ground surface. Soil–pile interaction was modeled using a surface-to-surface contact approach with a master–slave formulation, accounting for both normal and tangential behaviors. Normal contact response was governed by compressive normal stress N, while tangential behavior before slip was modeled using Coulomb's friction law $\tau = \mu N$. The static friction coefficient μ is defined as $\mu = tan\left(\frac{2}{3}\varphi_f\right)$, where φ_f represents the soil's internal friction angle at each depth. Friction angles of 33° and 37° were assumed for the upper and lower soil layers, respectively, corresponding to friction coefficients of 0.40 for medium-dense soil and 0.46 for dense sand (Wang et al. 2019). The present study focuses on simulating and validating one of the experiments (Csp3) using two scaled Peak Ground Acceleration (PGA) levels 0.04 g and 0.60 g, based on the 1995 Kobe earthquake. Numerical simulations consider acceleration time histories and 5%-damped spectral response and use the significant duration ($D_{5–95\%}$) to enhance computational efficiency (Figure 1).

5 FE SIMULATION RESULTS

5.1 *Soil responses*

Figure 3 presents the depth profiles of maximum deviatoric strain $\varepsilon_{q,max}$ and peak excess pore water pressure (EPWP) ratio $r_{u,max}$ for two levels of seismic excitation: PGA = 0.04g and PGA = 0.6 g. in distance of about 12 m from the pile center. Deviatoric strain and peak EPWP ratio can be calculated based on Equation (1) and Equation (2).

$$\varepsilon_q = \sqrt{\frac{2}{9}((\varepsilon_1 - \varepsilon_2)^2 + (\varepsilon_1 - \varepsilon_3)^2 + (\varepsilon_2 - \varepsilon_3)^2)} \quad (1)$$

$$r_{u,max} = \frac{U_{e,max}}{\sigma'_{\mathrm{V}}} \quad (2)$$

Where, $\varepsilon_1, \varepsilon_2, \varepsilon_3$ are principal strains, $U_{e,max}$, is the maximum EPWP and σ'_{V} is the initial vertical effective stress. Simulation results are presented for three advanced constitutive soil models: SANISAND, HP+IGS, and MHP+IGS, with $r_{u,max}$ values compared against centrifuge test measurements. Deviatoric strain data for the soil deposits were not recorded during the centrifuge experiments and are therefore evaluated solely through numerical predictions. Under low seismic intensity (PGA = 0.04g), the SANISAND model predicts a smaller peak deviatoric strain ($\varepsilon_{q,max} = 0.16\%$) compared to the HP+IGS ($\varepsilon_{q,max} = 0.68\%$) and MHP+IGS ($\varepsilon_{q,max} = 0.45\%$) models. As the seismic intensity increases, the SANISAND model continues to predict lower deviatoric strains relative to the hypoplastic-based models. Notably, SANISAND better captures the variation in strain response associated with changes in relative density, transitioning from medium-dense to dense soil layers. In contrast, the higher deviatoric strains predicted by the hypoplastic models may result from differences in how shear stiffness is computed at various depths, potentially leading to overestimation of nonlinearity in regions of lower effective stress. Under the ground motion with PGA = 0.04 g, the variation of EPWP with depth shows that both SANISAND and HP+IGS tend to overpredict pore water pressure compared to the centrifuge test data. These two models even predict liquefaction near the surface, which is not observed in the experimental results. In contrast, MHP+IGS better controls the buildup of EPWP and shows predictions that are in closer agreement with the test data, particularly in the upper soil layers. As the earthquake intensity increases to PGA = 0.6 g, there is a rapid rise in EPWP during the initial loading cycles. Under this higher intensity, the discrepancy between HP+IGS and MHP+IGS becomes less pronounced, especially in the dense soil layers, where HP+IGS provides predictions comparable to those of MHP+IGS. However, in the medium-dense layers, HP+IGS still significantly overestimates the peak EPWP ratio $r_{u,max}$ indicating limitations in capturing

liquefaction behavior accurately in those zones. To better understand the performance of different soil models under seismic loading, the response of soil elements on one side of the pile axis was evaluated using contour plots of peak deviatoric strain $\varepsilon_{q,max}$ and peak pore pressure ratio $r_{u,max}$. Figure 4 and Figure 5 demonstrate the contour results for peak deviatoric strain and EPWP ratio under seismic input motions with PGA values of 0.04 g and 0.6 g, respectively. As shown, the SANISAND model results in lower overall deviatoric strain levels, with high strain concentrations primarily localized near the pile. This suggests that the elevated strain near the pile is mainly due to the stress transfer from the pile to the surrounding soil. Away from the pile, the strain dissipates quickly, indicating limited influence in the far field. When comparing the HP+IGS and MHP+IGS models, the MHP+IGS model predicts slightly lower deviatoric strains, particularly in the medium-dense soil layers, suggesting improved strain control under cyclic loading. Regarding pore pressure buildup, both SANISAND and HP+IGS exhibit considerable excess pore pressure and are unable to control effective stress degradation during seismic analysis. In contrast, the MHP+IGS model shows a reduced liquefaction potential at both levels of seismic intensity. This performance of the MHP+IGS model can be attributed to a key modification in the hypoplastic formulations, the deactivation of the nonlinear component of the constitutive model during the initial stages of loading. This mechanism appears to delay the onset of excess pore pressure accumulation and leads to more stable stress conditions.

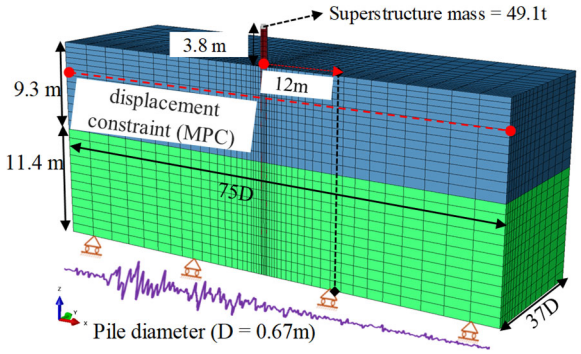

Figure 2. Schematic of the numerical simulation of SPSI, including geometry, boundary conditions, and instrumentation from the centrifuge tests.

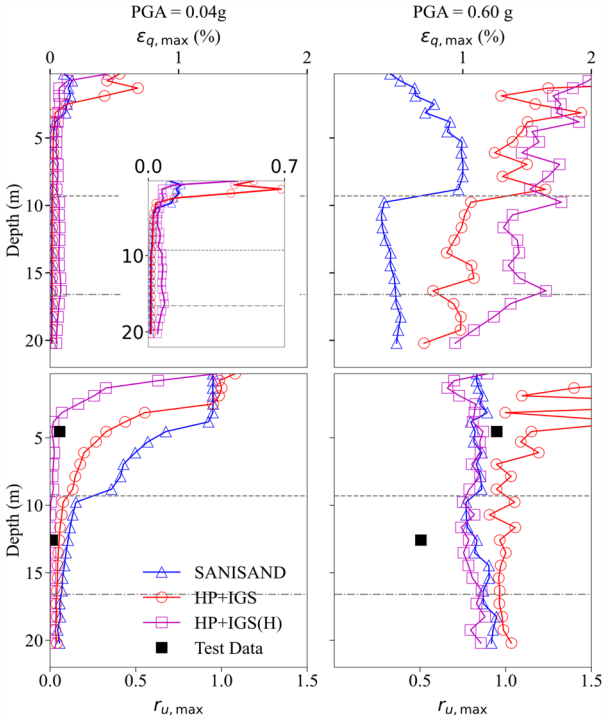

Figure 3. Variation of peak deviatoric strain and excess pore water pressure with soil depth, based on predictions from advanced constitutive models compared with test data at a distance of 12 m from the pile center (test data from Wilson, 1998).

5.2 *Pile responses*

Figure 6 shows the variation profile of the maximum bending moment induced in normalized pile depths during dynamic analysis. The results indicate that under slight earthquake intensity (PGA = 0.04 g), the SANISAND model predicts good agreement with the experimental data (Figure 6 (a)). In contrast, the hypoplastic models tend to underestimate the maximum bending moment in the upper part of the pile, and they also predict its location slightly lower than that predicted by the SANISAND model. At greater depths, the hypoplastic model predictions show an inverse trend. This change in the predicted bending moment behavior can be attributed to the increased deformation of the soil elements near the pile, as observed in the deviatoric strain contours. Figure 6 (b). illustrates the performance of different soil models in predicting the maximum bending moment profiles under seismic loading with a peak ground acceleration (PGA) of 0.6 g. The results indicate that the SANISAND and modified hypoplastic (MHP+IGS) models capture the maximum moment well along the pile depth. In contrast, the HP+IGS model underestimates the bending moment, likely due to significant soil stiffness degradation near the pile compared to the other two models. Figure 6 (c). compares simulation results with experimental data, showing that the modified hypoplastic model enhances prediction accuracy under high-intensity seismic loading. However, under low-stress-level loading, its predictive capability remains limited.

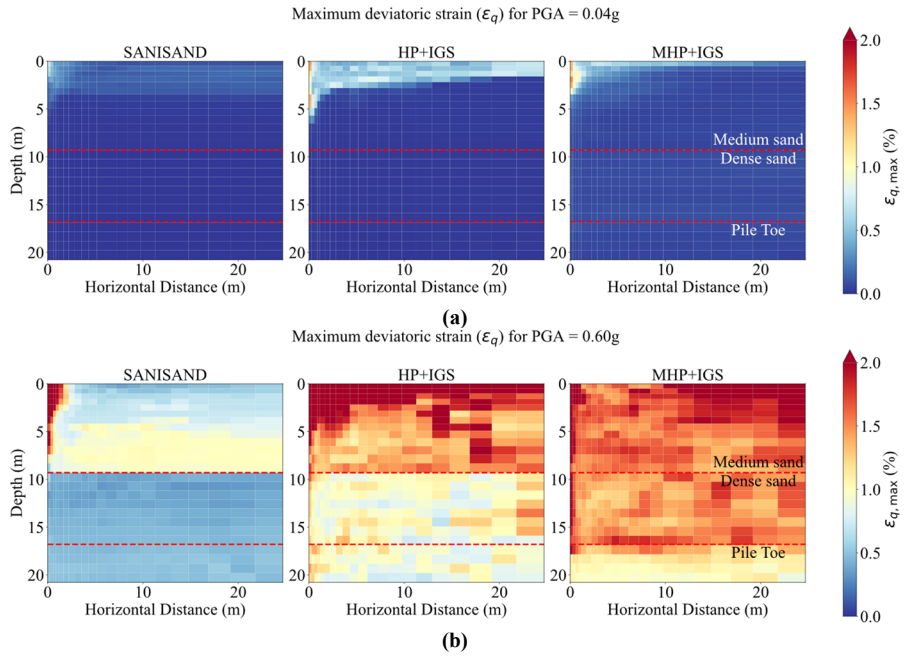

Figure 4. Contour plot of the maximum deviatoric strain response during seismic analysis: (a) PGA = 0.04 g; (b) PGA = 0.60 g.

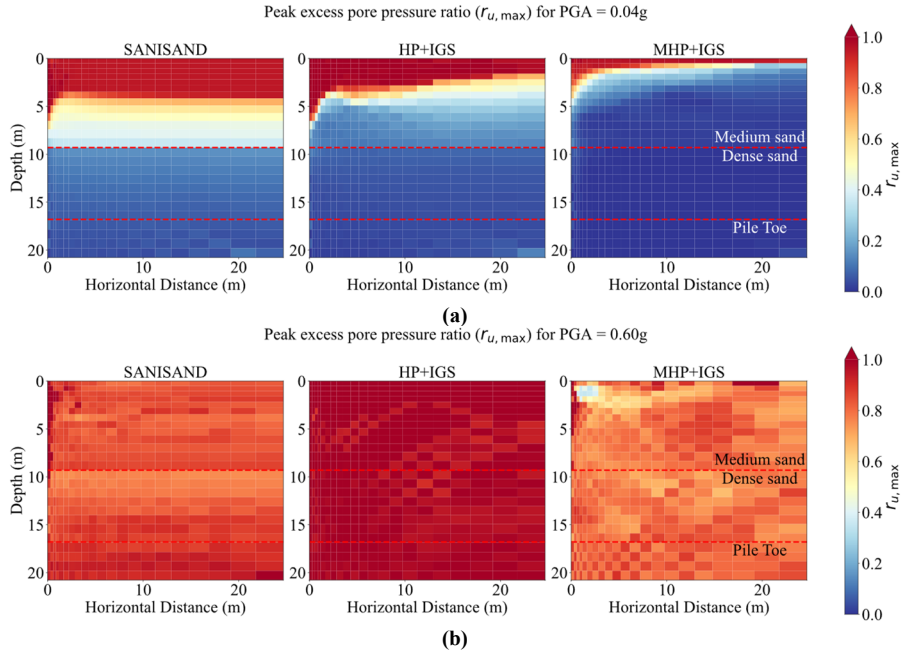

Figure 5. Contour plot of the peak EPWP ratio during seismic analysis: (a) PGA = 0.04 g; (b) PGA = 0.60 g.

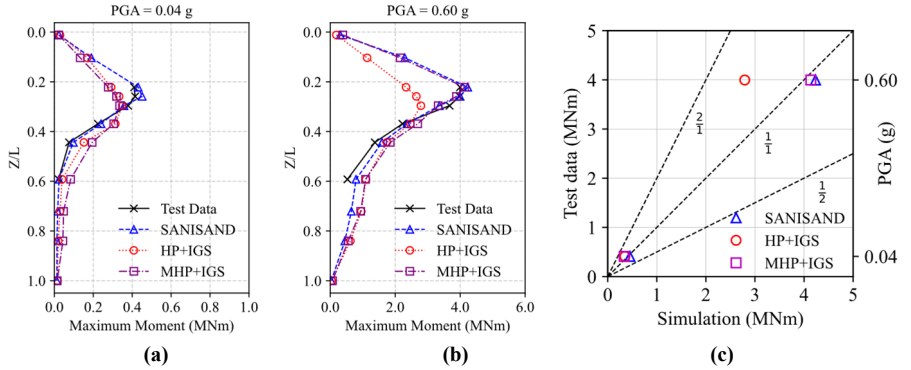

Figure 6. Maximum bending moment profile along normalized pile depth during seismic analysis: (a) PGA = 0.04 g; (b) PGA = 0.60 g; (c) comparison of the maximum response from simulation results with test data, test data from Wilson (1998).

6 SUMMARY AND CONCLUSIONS

This study evaluates the performance of various advanced constitutive models within a numerical framework in order to accurately represent the fully nonlinear behavior of the SPSI system during earthquake excitation. The SPSI response was investigated through numerical simulations using Abaqus finite element software under two scaled ground motions from the Kobe earthquake. The credibility of the simulation framework is ensured by validating the finite element model against a centrifuge test previously described by Wilson (1998). The primary goal of this research is to assess how effectively advanced constitutive soil models can capture the nonlinear response of soil subjected to seismic loading. To improve the accuracy of modeling under cyclic conditions, we introduce a combination of a modified hypoplastic model with the intergranular strain concept. This model is referred to as MHP+IGS (Liao et al., 2024; Niemunis & Herle, 1997). Model input parameters are calibrated using results from undrained monotonic and cyclic triaxial compression tests to replicate nonlinear soil responses. SANISAND, HP+IGS, and MHP+IGS, all three advanced soil models, are implemented in Abaqus through a user-defined material (UMAT) subroutine. We compared simulation results with centrifuge test data to evaluate the predictive performance of each model in terms of deviatoric strain, EPWP buildup, and bending moment response at the pile depth. The SANISAND model accurately predicts pile response and provides a reliable deviatoric strain distribution. However, it overestimates pore pressure variation, especially under low-intensity seismic loading. The HP+IGS model indicates deficiencies in predicting bending moments along the pile depth, primarily due to the overestimation of deviatoric strain near the pile. In comparison, the MHP+IGS model shows better accuracy in predicting how pore pressure builds up and how bending moments change, especially during strong ground shaking (PGA = 0.6 g). These findings demonstrate the potential of the MHP+IGS model to more reliably capture the seismic responses of soil–pile–structure interaction systems.

7 ACKNOWLEDGEMENTS

Support for this study was provided by the Austrian Research Promotion Agency (FFG), Project No. FO999898870. This study is part of a PhD thesis. The research of the second author was funded in part by the Austrian Science Fund (FWF) 10.55776/V918. The authors are grateful to Dr. Andrzej Niemunis for the development of the Incremental Driver (used for calibration) and to the developers of the UMAT of sand hypoplasticity (Fuentes and Triantafyllidis, 2015) and SANISAND (Dafalias & Manzari, 2004) that they have kindly made their resources available on the platform SoilModels.com. The UMAT of hypoplasticity was further extended by the first author of this paper.

8 REFERENCES

Dassault Systèmes, 2020. ABAQUS: theory and analysis user's manual, version 2020.

Dafalias, Y.F. and Manzari, M.T., 2004. Simple plasticity sand model accounting for fabric change effects. *Journal of Engineering Mechanics*, 130(6), pp.622–634. https://doi.org/10.1061/(ASCE)0733-9399(2004)130:6(622)

Fuentes, W. and Triantafyllidis, T., 2015. ISA model: a constitutive model for soils with yield surface in the intergranular strain space. *International Journal for Numerical and Analytical Methods in Geomechanics*, 39(11), pp.1235–1254. https://doi.org/10.1002/nag.2370

Joneidi, M., Medicus, G., Shafieiganjeh, R., Bathaeian, I. and Schneider-Muntau, B., 2025. Advanced soil constitutive models for predicting soil-pile-superstructure interaction: Evaluating liquefiable soil behavior under monotonic, cyclic, and seismic loading. Acta Geotechnica, 15(2827):23, https://doi.org/10.1007/s11440-025-02827-0

Kolymbas, D., 1977. A rate-dependent constitutive equation for soils. *Mechanics Research Communications*, 4, pp.367–372. https://doi.org/10.1016/0093-6413(77)90056-8

Lascarro, C., Tafili, M., Fuentes, W. and Duque, J., 2024. Comparative analysis of two intergranular strain-based hypoplastic models through elemental and centrifuge testing. *Soil Dynamics and Earthquake Engineering*, 180, p.108572. https://doi.org/10.1016/j.soildyn.2024.108572

Liao, D., Hu, X., Wang, S. and Zhou, C., 2024. Improvement of a hypoplastic model for sand under undrained loading conditions. *Canadian Geotechnical Journal*. https://doi.org/10.1139/cgj-2023-0670

Machaček, J., Staubach, P., Tafili, M., Zachert, H. and Wichtmann, T., 2021. Investigation of three sophisticated constitutive soil models: From numerical formulations to element tests and the analysis of vibratory pile driving tests. *Computers and Geotechnics*, 138, p.104276. https://doi.org/10.1016/j.compgeo.2021.104276

Niemunis, A. and Herle, I., 1997. Hypoplastic model for cohesionless soils with elastic strain range. *Mechanics of Cohesive-Frictional Materials*, 2(4), pp.279–299. https://doi.org/10.1002/(SICI)1099-1484(199710)2:4%3C279::AID-CFM29%3E3.0.CO;2-8

Petalas, A.L., Dafalias, Y.F. and Papadimitriou, A.G., 2020. SANISAND-F: Sand constitutive model with evolving fabric anisotropy. *International Journal of Solids and Structures*, 188, pp.12–31. https://doi.org/10.1016/j.ijsolstr.2019.09.005

Reyes, A., Taiebat, M. and Dafalias, Y.F., 2025. Modification of SANISAND-MSf model for simulation of undrained cyclic shearing under nonzero mean shear stress. *Journal of Geotechnical and Geoenvironmental Engineering*, 151(7), p.04025051. https://doi.org/10.1061/JGGEFK.GTENG-12658

Tafili, M., Duque, J., Mašín, D. and Wichtmann, T., 2024. A hypoplastic model for pre- and post-liquefaction analysis of sands. *Computers and Geotechnics*, 171, p.106314. https://doi.org/10.1016/j.compgeo.2024.106314

Taiebat, M., Jeremić, B., Dafalias, Y.F., et al., 2010. Propagation of seismic waves through liquefied soils. *Soil Dynamics and Earthquake Engineering*, 30, pp.236–257. https://doi.org/10.1016/j.soildyn.2009.11.003

Von Wolffersdorff, P.A., 1996. A hypoplastic relation for granular materials with a predefined limit state surface. *Mechanics of Cohesive-Frictional Materials*, 1(3), pp.251–271. https://doi.org/10.1002/(SICI)1099-1484(199607)1:3%3C251::AID-CFM13%3E3.0.CO;2-3

Wang, X., Ye, A. and Ji, B., 2019. Fragility-based sensitivity analysis on the seismic performance of pile-group-supported bridges in liquefiable ground undergoing scour potentials. *Engineering Structures*, 198, p.109427. https://doi.org/10.1016/j.engstruct.2019.109427

Wilson, D.W., 1998. *Soil-pile-superstructure interaction in liquefying sand and soft clay*. Davis: University of California.

Yang, M., Taiebat, M. and Dafalias, Y.F., 2022. SANISAND-MSf: a sand plasticity model with memory surface and semifluidised state. *Géotechnique*, 72(3), pp.227–246. https://doi.org/10.1680/jgeot.19.P.363